



1 Article

2 Synthesis of Chromium(II) Complexes with

3 Chelating Bis(alkoxide) Ligand and Their Reactions

4 with Organoazides and Diazoalkanes

- 5 Sudheer S. Kurup ¹, Richard J. Staples ², Richard L. Lord ^{3,*} and Stanislav Groysman ^{1,*}
- Department of Chemistry, Wayne State University, 5101 Cass Ave., Detroit, MI 48202, USA;
 sudheer.kurup@wayne.edu
- Department of Chemistry, Michigan State University, 578 S Shaw Ln, East Lansing, MI 48824, USA;
 staples@chemistry.msu.edu.
- Department of Chemistry, Grand Valley State University, 1 Campus Dr, Allendale, MI 49401, USA
- 11 * Correspondences: lordri@gvsu.edu (R.L.L.); groysman@wayne.edu (S.G.)
- 12 Academic Editor:

14

15

16

17

18

19

20

21

22

23

24

25

26

27

28

29

30

31

Received: date; Accepted: date; Published: date

Abstract: Synthesis of new chromium(II) complexes with chelating bis(alkoxide) ligand [OO]^{Ph} $(H_2[OO]^{Ph} = [1,1':4',1''-terphenyl]-2,2''-diylbis(diphenylmethanol))$ and their subsequent reactivity in the context of catalytic production of carbodiimides from azides and isocyanides are described. Two different Cr(II) complexes are obtained, as a function of the crystallization solvent: mononuclear Cr[OO]^{Ph}(THF)2 (in toluene/THF) and dinuclear Cr2([OO]^{Ph})2 (in CH2Cl2/THF). The electronic structure and bonding in Cr[OO]^{Ph}(THF)₂ were probed by DFT calculations. Isolated Cr2([OO]Ph)2 undergoes facile reaction with 4-MeC6H4N3, 4-MeOC6H4N3, or 3,5-Me2C6H3N3 to yield diamagnetic Cr(VI) bis(imido) complexes; a structure of Cr[OO]Ph(N(4-MeC₆H₄))₂ was confirmed by X-ray crystallography. The reaction of Cr2([OO]Ph)2 with bulkier azides N3R (MesN3, AdN3) forms paramagnetic products, formulated as Cr[OO]^{Ph}(NR). The attempted formation of a Cr-alkylidene complex (using N2CPh2) forms instead chromium(VI) bis(diphenylmethylenehydrazido) complex Cr[OO]Ph(=NNCPh2)2. Catalytic formation of carbodiimides was investigated for the azide/isocyanide mixtures containing various aryl azides and isocyanides. The formation of carbodiimides was found to depend on the nature of organoazide: whereas bulky mesityl led to the formation of carbodiimides with all isocyanides; no carbodiimide formation was observed for 3,5-dimethylphenylazide or 4-methylphenylazide. of $Cr_2([OO]^{Ph})_2$ or $H_2[OO]^{Ph}$ with NO^+ leads to the [1,2-b]-dihydroindenofluorene, likely obtained via carbocation-mediated cyclization of the ligand.

Keywords: alkoxides; azides; carbodiimides

32 33

34

35

36

37

38

39

40

41

42

43

1. Introduction

Organoazides constitute efficient and sustainable precursors for the formation of reactive nitrene functionality, which engenders many useful transformations, including C-H bond amination, aziridination, formation of azoarenes and carbodiimides, and others [1–7]. Transition metals generally enable milder conditions for the formation of nitrenes and higher selectivity in their subsequent transfer. The majority of nitrene-transfer studies are focused on middle and late transition metals, which generally feature weaker metal-imido bonds and therefore exhibit more reactive nitrene functionalities [8–21]. In contrast, early transition metals (particularly chromium) typically exhibit less reactive nitrene functionalities due to the stability of multiple metal-nitrogen bonds [22–28]. However, recent studies demonstrated the ability of coordinatively unsaturated

44 chromium(IV)-imido to transfer nitrene to olefins or isocyanides to form aziridines and 45 carbodiimides, respectively [29-31]. C-C and C-H bond activation reactions featuring reactive 46 chromium(IV) imido were also reported [32]. As part of our ongoing investigation of nitrene- and 47 carbene-transfer chemistry mediated by 3d complexes in bulky alkoxide ligand environments 48 [33,34], we have reported synthesis and reactions of chromium-imido complexes featuring two 49 bulky monodentate alkoxides [OC[†]Bu₂Ph] [31]. We have demonstrated that Cr^{IV}(OC[†]Bu₂Ph)₂(NR[′]) 50 complexes, which were formed for bulky R' groups (R' = Mes, 2,6-Et₂C₆H₃, Ad) enabled catalytic 51 transfer of nitrene group [NR'] to isocyanides to form carbodiimides. In contrast, the reaction of less 52 bulky para-substituted aryl azides N₃R' (R' = 4-MeC₆H₄, 4-MeOC₆H₄, 4-CF₃C₆H₄) formed Cr(VI) 53 complexes CrVI(OR)2(NR')2 which were catalytically inactive. Recently, we have reported a new 54 chelating bis(alkoxide) ligand [OO]^{Ph} [35], that created similar bis(alkoxide) ligand environment but 55 warranted higher degree of stability of the resulting iron complex Fe[OO]^{Ph}, and consequently led to 56 a broader range of catalytic nitrene transfer compared with related Fe(OR)2 systems [36,37]. Herein 57 we report our synthetic, structural, and catalytic studies on the chemistry of Cr^{II}[OO]^{Ph} with 58 organoazides and diazoalkanes, and compare this reactivity with the previously reported 59 $Cr^{II}(OC^tBu_2Ph)_2$ system.

2. Results and Discussion

60

61

62

63

64

65

66

67 68

69

70

71

72

2.1. Synthesis and Structures of Cr(II) Precursors

Treatment of the chromium(II) amide precursor with one equivalent of H₂[OO]^{Ph} in THF produces a green solid. Recrystallization of the product from toluene/THF mixture yields pale green Cr[OO]Ph(THF)2 mononuclear **(1)** related to the mononuclear Cr(OC^tBu₂(3,5-Ph₂Ph))₂(THF)₂ [38]. In contrast, recrystallization of the product from a mixture of two polar solvents (CH₂Cl₂ and THF) forms pale green-blue homodinuclear complex Cr₂[OO]^{Ph}₂ (2, Scheme 1) isolated in 79% yield. Homodinuclear complex 2 is structurally related to the previously alkoxide-bridged $Cr_2(OC^tBu_2Ph)_4$ [31], $Cr_2(OC^tBu_3)_2(\mu^2-OC^tBu_2H)_2$ siloxide-bridged Cr₂(OSi⁴Bu₃)₄ [40]. We note that monodentate alkoxides [OC⁴Bu₂Ph] and [OC¹Bu₂(3,5-Ph₂Ph)] formed dinuclear or mononuclear complexes selectively [31,38], whereas the chelating ligand appears to support both types of geometries in the solid state, depending on the nature of the crystallization medium.

$$\begin{array}{c} Ar = 4.\text{MeCo}_{c}H_{1}, 3\\ Add = 4.\text{MeCo}_{c}H_{1}, 4\\ Add = 4.\text{MeCo}_{c}H_{2}, 4\\ Add = 4.\text{$$

Scheme 1. Synthesis and reactivity of Cr(II) complex in the chelating bis(alkoxide) ligand environment.

The structures of complexes 1 and 2 are given in Figure 1. The structure of 1 is similar to the previously reported structure of Fe[OO]^{Ph}(THF)₂ [35]. However, the structure of Fe[OO]^{Ph}(THF)₂ exhibited very long distance between the metal and the central phenyl (>3 Å) indicating no interaction [35]. In contrast, the distance between the chromium center and the central phenyl in 1 is 2.49(1) Å, which suggests bonding between the metal and the phenyl ring. The inter-alkoxide RO-Cr-OR and THF-Cr-THF angles are 173.6(2) ° and 88.1(2) °, respectively. Two independent molecules of homodinuclear complex 2 were found in the asymmetric unit exhibiting similar structural parameters; only one is shown. Each $[OO]^{Ph}$ ligand provides one terminal and one bridging alkoxide donor; no coordination to the central phenyl is observed in this case $(Cr---Ph \ge 3.0 \text{ Å})$. While the overall geometry and metrics in 2 are similar to those of $Cr_2(OC^tBu_2Ph)_4$ and related complexes [32,39,40], the metal centers in 2 exhibit significant distortion of trigonal planar geometry as indicated by the considerable difference in O-Cr-O angles (Figure 2) and displacement of Cr from the trigonal plane (varies between 0.105–0.348 Å).

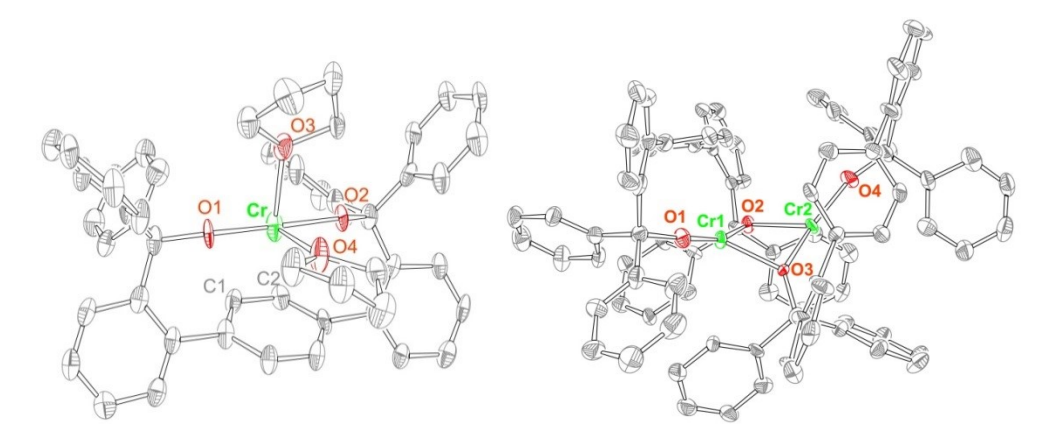


Figure 1. X-ray structures of **1** (left) and **2** (right), 50% probability ellipsoids. H atoms and co-crystallized solvent molecules were omitted for clarity. Selected bond distances (Å) and angles (°)

> 96 97

> 98

99

100

101

102

103

104

105

106

107

108

109

110

111

112

113

114

115

116

117

118

119

120

121

122

91

for 1: Cr O1, 1.924(6), Cr O2, 1.935(6), Cr O3, 2.156(7), Cr O4, 2.277(6), Cr --- Ph 2.49(1), O1 Cr1 O2, 173.6(2), O1 Cr1 O3, 86.7(2), O2 Cr1 O3, 90.0(3), O1 Cr1 O4, 85.9(2), O2 Cr1 O4, 88.5(2), O3 Cr1 O4, 88.1(2). Selected bond distances (Å) and angles (°) for 2: Cr1 O1, 1.788(5), Cr2 O4, 1.799(5), Cr1 O2, 1.976(5), Cr1 O3, 2.013(6), Cr2 O3, 1.981(5), Cr2 O2, 2.049(5), Cr1 --- Cr2, 2.896(2), O2 Cr1 O3, 81.2(2), O1 Cr1 O2, 150.2(3), O1 Cr1 O3, 120.1(2).

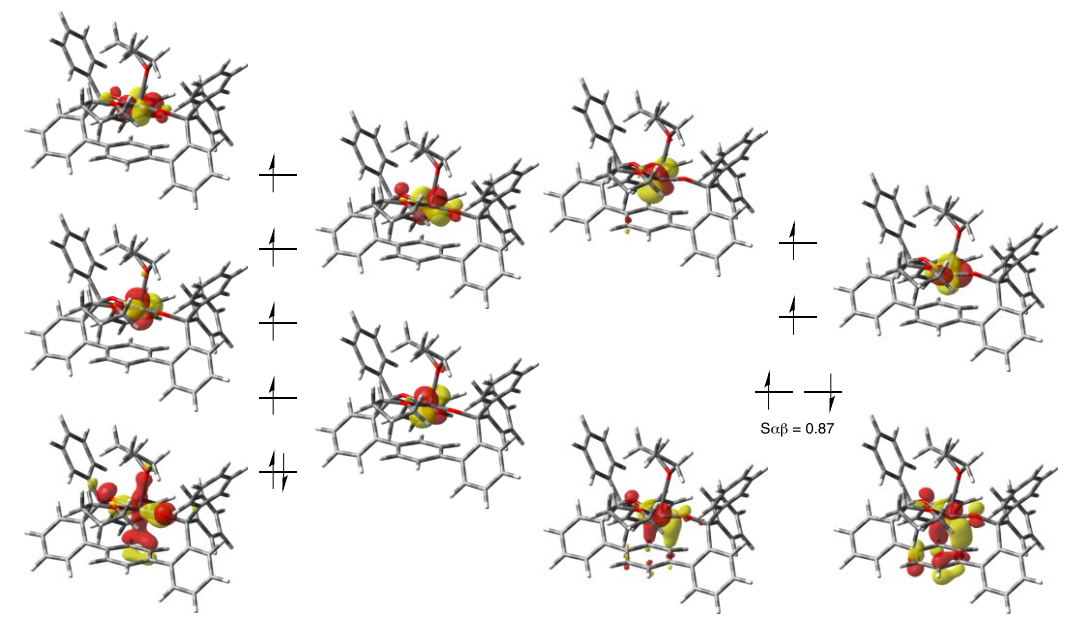
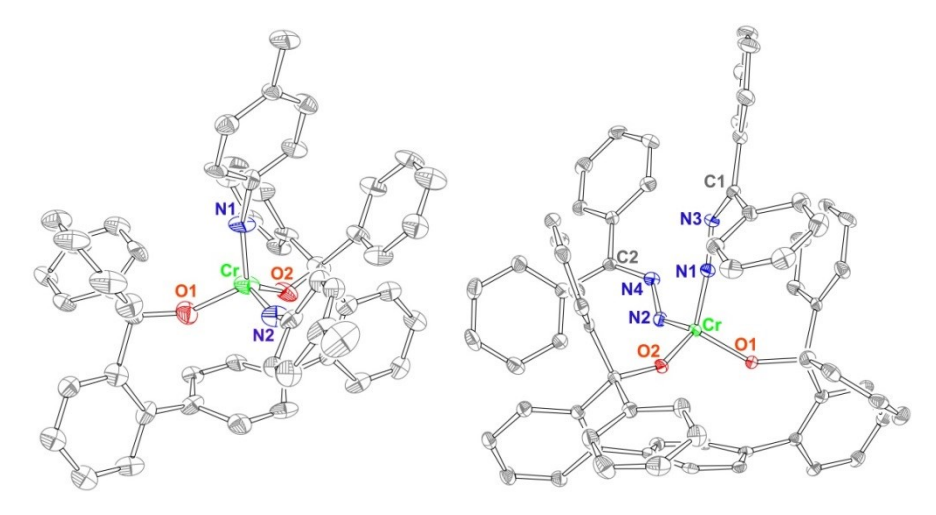


Figure 2. Corresponding orbital diagrams for $\mathbf{1}_Q$ (left) and $\mathbf{1}_T$ (right) at the BP86-D3/def2-SVP level of theory. Orbitals are plotted with an isosurface value of 0.05 au.

To better understand the electronic structure and bonding in 1, DFT calculations were performed. Singlet (1s), triplet (1r), and quintet (1q) states were optimized. 1q is lowest in free energy, followed by 1_T at 19.7 kcal/mol, and 1s at 28.6 kcal/mol. The optimized structure of 10 agrees well with the crystallographically determined structure and has bond lengths of Cr-O1 = 1.915 Å, Cr–O2 = 1.928 Å, Cr–O3 = 2.203 Å, Cr–O4 = 2.281 Å, Cr–C1 = 2.475 Å, and Cr–C2 = 2.525 Å; both 1_T and 1s are inconsistent with the x-ray data (Table S1, SI). Based on the spin density localized at Cr, 10 is best described as a high-spin Cr(II) species. Similar to what was observed in the optimization of different spin states of Fe[OO] $^{Ph}(THF)_2$ [35], the higher-energy, lower spin states $1\tau/1s$ exhibit much shorter Cr-phenyl contacts of 2.1-2.2 Å. Mayer bond orders for Cr-C1/C2 are calculated to be 0.25 and 0.23 in 1_Q. In comparison, quintet Fe[OO]^{Ph}(THF)₂ (with Fe–C distances of 2.8–2.9 Å) has smaller bond orders of 0.06 and 0.09, whereas 1_T has larger bond orders of 0.64 and 0.65. For perspective, M-Other bond orders are 0.2–0.3 and the M-Oalkoxide bond orders are 0.6–0.9. Frontier orbital diagrams of 10 and 1T (Figure 2) illustrate the Cr-phenyl bonding in both spin states. The much stronger bonding in 1[™] is due to the d-\overline{o} backbonding that is possible with intermediate-spin Cr(II) ion. This back-bonding is not significant in 10 due to half-occupation of that d-orbital in the high-spin Cr(II) ion. Collectively, these computational data suggest a weak covalent interaction between Cr and the bridging phenyl moiety in 1.

We have also investigated the structures of **1** and **2** in solution. Both compounds give rise to paramagnetic NMR spectra, as anticipated. The UV-vis spectra of **1** and **2** (collected in THF) are very similar, exhibiting a peak around 710 nm, and a shoulder around 510 nm (Figures S39 and S40, SI). The solution magnetic moment of **1** (3.0(3) μ B, C₆D₆) was found to be significantly lower than the expected spin-only value of 4.9 μ B. Recalculated for the structure of Cr₂([OO]^{Ph})₂, the observed magnetic moment is 2.6(2) μ B (per Cr), that is close to the observed value of 2.5(3) μ B reported for Cr₂(OC⁴Bu₂Ph)₂ [31]. These data suggest that **1** undergoes dimerization in solution to form **2**.

Following the synthesis of the chromium(II) precursor, its reactivity with organoazides was investigated. Complex 2 was utilized as a precursor in group-transfer reactions. Similar to Cr₂(OC²Bu₂Ph)₄ [31], 2 was found to exhibit profoundly distinct reactivity with non-bulky (4-tolyl, 4-methoxyphenyl, and 3,5-dimethylphenyl) vs. bulky (mesityl, adamantyl) organoazides. Treating a green solution of 2 with two equivalents of para-tolylazide in THF leads to a dark-brown solution, from which diamagnetic 3 is isolated in 69% yield by recrystallization from THF/ether. Similarly, treating 2 with two equivalents of 4-MeOC₆H₄N₃ or 3,5-Me₂C₆H₃N₃ forms brown solutions containing diamagnetic products 4 and 5 in 54% and 59%, respectively. We were not able to obtain X-ray quality crystals of 4 and 5, however, their NMR and UV-Vis data (see SI) suggests close similarity to 3. The overall connectivity of 3 was confirmed by X-ray structure determination (Figure 3). The structure reveals distorted tetrahedral geometry, consistent with Cr(VI) bis(imido) formulation. No chromium-phenyl interaction is observed in this case, with the chromium-phenyl distance exceeding 3.5 Å. As the structure was of relatively low quality, its metric parameters will not be further discussed.



138 139

140

141

142

124

125

126

127

128

129

130

131

132

133

134

135

136

137

Figure 3. X-ray structure of 3 (left) and 6 (right), 50% probability ellipsoids. H atoms and co-crystallized solvent molecules were omitted for clarity. Selected bond distances (Å) for 6: Cr O1 1.807(2), Cr O2 1.777(2), Cr N1 1.645(3), Cr N2 1.716(3), N1 N3 1.305(4), N2 N4 1.301(4). Selected bond angles (°): O2 Cr O1 110.0(1), N1 Cr N3 99.7(2), N1 Cr O2 110.5(1), N2 Cr O2 109.2(1), N1 Cr O1 113.1(1), Cr N1 N3 159.8(2), Cr N2 N4 131.2(2).

143 144 145

146

147

148

149

150

151

152

153

In contrast, the reaction of the chromium(II) precursor with two equivalents of bulkier mesityl azide (per Cr) produces a paramagnetic brown solution, containing approximately one equivalent of unreacted azide. Similarly, treating chromium(II) precursor with two equivalents of adamantyl azide also produces paramagnetic product, along with unreacted azide. We were not able to obtain X-ray quality crystals of the products. The formation of trigonal Cr(IV) mono(imido) complexes is proposed, based on similar formation of brown paramagnetic Cr^{IV}(OC¹Bu₂Ph)₂(NMes) and Cr^{IV}(OC¹Bu₂Ph)₂(NAd) upon reaction of [Cr(OC¹Bu₂Ph)₂] with excess azide. We note that selective formation of Cr(IV) mono(imido) complexes upon reaction with bulkier organoazides was also observed for the chromium(II) system ligated by two monodentate siloxides, [Cr(OSi^tBu₃)₂] [40].

154 155 156

In addition to the reactions of Cr(II) precursor with organoazides, we have also studied its reactivity with azobenzene, with the goal to produce Cr(VI) bis(imido) via azobenzene cleavage. Cleavage of the N=N double bond in azoarenes at a single metal center is rare [41-44]. Heating the mixture of complex 2 with azobenzene to 60 °C in C₆D₆ for 24 h did not lead to the formation of Cr^{VI}[OO]^{Ph}(NPh)₂ as indicated by ¹H NMR spectroscopy.

157

Next, the reactivity of the Cr(II) bis(alkoxide) precursor with diazoalkanes was investigated, targeting formation of Cr(IV)/Cr(VI)-alkylidene complexes. Cr-alkylidene complexes are rare [26,45,46], and their reactivity is relatively unexplored. The related cobalt(II) bis(alkoxide) complex Co(OC^tBu₂Ph)₂(THF)₂ formed high-valent cobalt-alkylidene upon reaction with N₂CPh₂ and

N₂C(Ph)(CO₂Me) [47], whereas the corresponding iron complex Fe(OC²Bu₂Ph)₂(THF)₂ reductively coupled diazoalkanes/diazoesters via terminal nitrogens to form bridging tetrazene species [48]. Different reactivity mode was observed for the chromium bis(alkoxide). Treatment of **2** with diphenyldiazomethane results in the formation of brown Cr[OO]^{Ph}(NNCPh₂)₂ species (**6**), which was characterized by X-ray crystallography. The complex appears unstable in both solid state and solution. Our repeated attempts to collect NMR spectrum on the X-ray quality crystals produced spectra with varying but significant number of decomposition products (benzophenone azine, free ligand); peaks attributable to the complex were broad and not informative. Wolczanski and coworkers have reported similar reactivity of Cr₂(OSi⁴Bu₃)₄ with N₂CPh₂ to yield Cr(OSi⁴Bu₃)₂(N₂CPh₂)₂ complex [40]; their complex also demonstrated limited stability.

The structure of **6** and selected metrics are given in Figure 3. The chromium center exhibits distorted tetrahedral geometry. Interestingly, the Cr-N bonds are different, one being significantly shorter (1.645(3) Å) than the other (1.716(3) Å). The shorter bond could be indicative of the higher metal-nitrogen bond order (triple), while the longer one indicates metal-nitrogen double bond. The Cr-N-N bond angles of the [NNCPh₂] functionality are consistent with the above formulations: for the triply bonded [Cr=N1-N3] hydrazido, the angle is closer to linear $(159.8(2) ^{\circ})$, whereas for the doubly bonded [Cr=N2-N4] the angle is smaller $(131.2(2) ^{\circ})$. It is noted that the N1-N3 and N2-N4 bonds are similar (1.304(4) vs. 1.301(4) Å), being intermediate between single and double. Similar dependence of the Cr-N-N angle within diphenylmethylenehydrazido functionalities on the chromium-nitrogen bond order was reported by Wolczanski, Cundari and coworkers for the related Cr(OSi^tBu₃)₂(=N₂CPh₂)₂ [40]. The major difference between the present structure and the structure reported by Wolczanski is that in Cr(OSi^tBu₃)₂(=N₂CPh₂)₂ the Cr-N bonds were similar (1.664(2) and 1.666(2) Å), leading to similar Cr-N-N bond angles $(150.2(2) \text{ and } 150.4(3) ^{\circ})$.

DFT calculations on 6 were performed to analyze the electronic structure of this species. Singlet (6s), triplet (6t), and quintet (6o) states were optimized and the singlet was found to be lowest in free energy followed by the triplet (+15.1 kcal/mol) then the quintet (+33.9 kcal/mol). Only the optimized structure of 6s is consistent with the experimental x-ray structure (Table S3, SI) and has no unpaired electrons. As the localized frontier orbitals in Figure 4 demonstrate, there are two @-bonding interactions with the more linear diazoalkane ligand (HOMO-1/LUMO+3, HOMO-3/LUMO) compared to one with the less linear diazoalkane ligand (HOMO/LUMO+4), though the HOMO-1/LUMO+3 pair shows interaction with both diazoalkane ligands. The modest difference in Mayer bond orders of 1.61 vs. 1.52 for Cr–N1 vs. Cr–N2 suggests that both Cr–N bonds are between doubly and triply bonded, but that bonding to N1 is stronger.

Figure 4. Frontier orbital diagram for **6**s at the BP86-D3/def2-SVP level of theory. Orbitals are plotted with an isosurface value of 0.05 au.

2.3. Reactivity of Cr(II) with CO, CNR, and NO+

Following the investigation of the reactivity of Cr(II) bis(alkoxide) precursor with organoazides and diazoalkanes, its reactivity with isocyanides, carbon monoxide, and nitrosonium was explored next. It was previously shown that $Cr_2(OC^tBu_2Ph)_4$ reacted with isocyanides to form $Cr^{II}(OC^tBu_2Ph)_2(CNR)_4$ (R = 2,6-Me₂C₆H₃); formation of $Cr^{II}(OC^tBu_2Ph)_2(CNR)_4$ enabled subsequent development of the catalytic cycle for the production of carbodiimides. Hoping that the more stable and sterically demanding chelating bis(alkoxide) system will enable better catalytic reactivity in CNR and perhaps CO transfer, reactions of $Cr[OO]^{Ph}$ with xylyl isocyanide and carbon monoxide were investigated. The reactivity of nitrosonium ((NO)(BF₄)) were also studied, in light of the isoelectronic nature between NO⁺ and CO/CNR.

Addition of excess xylyl isocyanide to the light-green solution of 2 (dissolved in THF) forms brown solution immediately. ¹H NMR spectrum of the product indicates its paramagnetic nature. Although our multiple attempts to obtain X-ray quality crystals of the isocyanide product did not lead to fruition, UV-vis spectrum of the crude product is similar to the UV-vis spectrum of isolated Cr^{II}(OC^tBu₂Ph)₂(CN(2,6-Me₂C₆H₃))₄ (peaks around 400 and 460 nm, Figure S44) suggesting the similarity of the products. In contrast, no color change was observed after treating the solution of 2 in THF with CO. Subsequent recrystallization from toluene/THF mixture formed instead the crystals of compound 1, further confirming the lack of reactivity with CO.

The reaction of 2 with NO+ took an unexpected turn. Addition of (NO)(BF₄) to the green solution of 2 (THF) led to the development of cloudy yellow solution over the course of several hours. Subsequent recrystallization from THF yields colorless crystals of 6,6,12,12-tetraphenyl-6,12-dihydroindeno[1,2-b]fluorene 7 (Figure 5) isolated in 92% yield. The reaction course does not depend on the presence of Cr: treatment of the ligands precursor $H_2[OO]^{Ph}$ with (NO)(BF₄) yields the same product 7. Cyclization of terphenyl bis(carbinol)s via carbocation

intermediates to give various substituted dihydroindenofluorenes had been previously reported [49,50]. We surmise that the reaction proceeds via nitrosonium abstraction of hydroxyl (to yield nitrous acid) followed by cyclization as described in Scheme 2.

225226

227

222

223

224

Figure 5. X-ray structure of 7, 50% probability ellipsoids. H atoms and co-crystallized solvent molecules were omitted for clarity.

228229

230

231

232

233

234

235

236

237

238

239

240

241

242

243

244

245

246

247

248

Scheme 2. Cyclization mechanism of H₂[OO]^{Ph}.

2.4. Catalytic Reactivity in the Formation of Carbodiimides

Given the ability of the Cr^{II}[OO]^{Ph} precursor to undergo stoichiometric reactions with organoazides and isocyanides, we turned next to investigate its catalytic reactivity in formation of carbodiimides. A matrix of 4 representative aryl azides of varying steric bulk (mesityl, 2-methylphenyl, 3,5-dimethylphenyl, and 4-methylphenyl) and 4 representative isocyanides (xylyl, 4-methoxyphenyl, adamantyl, and cyclohexyl) was investigated (Scheme 3). All reactions were carried out in C₆D₆ at 60 °C for 24 h; the nature of the reaction products and their yields were determined by ¹H NMR spectroscopy. The outcome of the catalytic reaction appears to be a primary function of the organoazide nature. Catalytic formation of carbodiimides is observed for the bulkier mesityl azide. The reaction of mesityl azide with xylyl isocyanide gives nearly quantitative yield; good to moderate yields (72-50%) are observed for other isocyanides. For the ortho-monosubstituted 2-methylphenyl azide, the reaction with xylyl isocyanide produces carbodiimide in a good yield, whereas other isocyanides give low yields of the corresponding products. No carbodiimide formation is observed for 3,5-dimethylphenyl azide and 4-methylphenyl azide. These results are rationalized by the nature of the chromium-imido intermediate, as was described in our previous study [31]. Whereas bulkier azide forms a chromium(IV)-imido, which is capable of isocyanide coordination and subsequent N-C bind formation, tetrahedral chromium(VI) bis(imido) (formed with non-bulky aryl azides) does not coordinate an isocyanide and therefore does not catalyze N-C bond formation.

N=C=N-CV

CNR

Scheme 3. Catalytic formation of carbodiimides mediated by 2.

3. Materials and Methods

50%

3.1. General

249250

251

252

253

254

255

256

257

258

259

260

261

262

263

264

265

266

267

268

269

270

271

272

273

274

275

276

277

278

CrCl₂ and LiN(Si(CH₃)₃)₂ were purchased from Strem chemicals and Sigma-Aldrich, respectively, and used as received. Previously reported methods were used to synthesize Cr(N(SiMe₃)₂)₂(THF)₂ and the ligand precursor H₂[OO]^{Ph} [35,51]. Deuterated solvents were purchased from Cambridge Isotope Laboratories and stored over 3 Å molecular sieves. Non-deuterated solvents were purchased from Sigma-Aldrich chemicals and purified using MBraun solvent purification system. Characterization of compounds was carried out using ¹H and ¹³C NMR spectroscopy, high-resolution mass spectrometry and elemental analysis. Selected chemicals were characterized by X-ray crystallography. NMR spectra of carbodiimides and complexes were recorded using Agilent 400 MHz spectrometer and Agilent DD2 600 MHz spectrometer, respectively, in C6D6 at room temperature at Lumigen Instrument center. Chemical shifts and coupling constants (J) are reported in parts per million and Hertz, respectively. Elemental analysis analyses were carried out by Midwest Microlab LLC under air-free conditions. Thermo Fisher Scientific LTQ Orbittrap XL mass spectrometer at the Lumigen Instrument Centre was used for high resolution mass spectra. IR spectra of powdered samples were recorded on Shimadzu IR Affinity-1 FT-IR spectrometer outfitted with a MIRacle10 attenuated total reflectance accessory with a monolithic diamond crystal stage and pressure clamp. Shimadzu UV-1800 spectrometer was used to collect UV-visible spectra. All air-sensitive reactions were carried out in a nitrogen-filled glovebox.

3.2. Synthesis of Cr Complexes 1-6 and Compound 7

Cr₂([OO]^{Ph})₂ and Cr[OO]^{Ph}(THF)₂ (1 and 2). A solution of ligand precursor H₂[OO]^{Ph} (0.034 g, 0.057 mmol) in THF (5 mL) was added to a solution of Cr(N(SiMe₃)₂)₂(THF)₂ (0.030 g, 0.057 mmol) in THF (5 mL). The color of the reaction changed from purple to light green over a course of 4 h. The solvent was removed under vacuum and the resulting residue recrystallized in DCM-THF mixture at -35 °C to obtain light green crystals of 2 in 79% yield (0.029 g, 0.023 mmol). Anal. Calcd for C₈₈H₆₄Cr₂O₄: C, 81.97, H, 5.00. Found: C, 80.82, H, 6.23. λ_{max} (ϵ_{M} (L⁻¹ cm⁻¹ mol⁻¹)) 706 nm (28000). IR (cm⁻¹): 2947 (m), 2337 (m), 1334 (w), 1151 (w), 987 (m), 840 (m), 756 (s), 702 (s). A similar procedure was used to synthesize Cr[OO]^{Ph} (THF)₂ (1) but recrystallization was done in toluene with small

amount of THF. Calcd for C₅₂H₄₆CrO₄: C, 79.17, H, 6.13. Found C, 78.37, H, 5.39. IR (cm⁻¹) 2916 (m), 2353 (m), 1458 (m), 1365 (w), 1319 (w), 1149 (w), 1026 (m), 995 (w), 833 (m), 779 (s), 740 (m), 709 (m), 686 (m).

Synthesis of Cr[OO]^{Ph}(N(4-CH₃C₆H₄))₂ (3). A solution of 4-azidotoluene (0.020 g, 0.15 mmol) in THF was added to a 5 mL solution of Cr₂([OO]^{Ph})₂ (0.050 g, 0.038 mmol). Upon addition, the solution color changed from light green to brown; the release of N₂ was also observed. The reaction was stirred for 24 h. The solvent was removed under vacuum and the solid residue was recrystallized from ether-THF mixture at – 35 °C to afford dark brown crystals in 69% yield (0.046 g, 0.054 mmol). ¹H NMR (600 MHz, C₆D₆, 298 K): δ 7.58 (d, 2H, J_{HH} = 7.6 Hz, H_a), 7.6 (d, 8H, J_{HH} = 6.1 Hz, H_f), 7.41 (s, 4H, H_e), 7.10-7.12 (m, 2H, H_b), 7.03-7.07 (m, 12H, H_g & H_h), 6.93-6.96 (m, 4H, H_c & H_d), 6.53 (d, 4H, J_{HH} = 7.6 Hz, H_f, 6.15 (d, 4H, J_{HH} = 8.2 Hz, H_i), 1.92 (s, 6H, H_k). ¹³C NMR (150 MHz, C₆D₆, 298 K): δ 160.69, 151.19, 146.27, 142.97, 142.93, 137.30, 131.11, 130.92, 129.17, 128.22, 127.92, 127.55, 127.52, 127.37, 126.39, 125.57, 124.26, 95.51, 20.72.

Figure 6. Assignment of ¹H NMR signals for 3 (see previous paragraph for details).

Cr[OO]^{Ph}(N(4-CH₃OC₆H₄))₂ (4). A solution of 4-azidoanisole (0.023 g, 0.15 mmol in THF) was added to a 5 mL THF solution of Cr₂([OO]^{Ph})₂ (0.050 g, 0.038 mmol). Color changed from light green to brown with release of N₂ and the reaction was stirred for 24 h. The solvent was removed under vacuum and the resulting residue was recrystallized from ether/THF mixture at - 35 °C to give brown solid which was washed with ether to afford the product in 54% yield (0.54 g, 0.043 mmol). ¹H NMR (600 MHz, C₆D₆, 298 K): δ 7.57-7.61 (m, 10H, H_a and H_f), 7.44 (s, 4H, H_e), 7.10 - 7.12 (m, 2H, H_b), 7.02 - 7.08 (t, 8H, J_{HH} = 7.0 Hz, H_g), 7.01 - 7.03 (t, 4H, J_{HH} = 7.0 Hz, H_h), 6.97 (m, 4H, H_c and H_d), 6.31 (d, 4H, J_{HH} = 8.8 Hz, H_i), 6.27 (d, 4H, J_{HH} = 8.8 Hz, H_i), 3.07 (s, 6H, H_k). ¹³C NMR (150 MHz, C₆D₆, 298 K): δ 158.54, 157.54, 151.30, 146.41, 143.00, 131.08, 130.95, 129.21, 127.92, 127.71, 127.54, 127.52, 127.31, 126.32, 126.13, 125.54, 112.79, 95.07, 54.91.

Figure 7. Assignment of ¹H NMR signals for 4 (see previous paragraph for details).

Cr[OO]^{Ph}(N(3,5-Me₂C₆H₃))₂ (5). A solution of 3,5-dimethylphenyl azide (0.022 g, 0.15 mmol) in THF) was added to THF solution (5 mL) of Cr₂([OO]^{Ph})₂ (0.050 g, 0.038 mmol). Color changed from light green to brown with release of N₂ and the reaction was stirred for 24 h. The solvent was removed under vacuum and the residue was recrystallized from ether-THF at – 35 °C to form brown solid which was washed with ether to afford the product in 57% (0.038 g, 0.043 mmol). ¹H NMR (600 MHz, C₆D₆, 298 K) δ 7.57 - 7.61 (m, 10H, H_a and H_f), 7.42 (s, 4H, H_e), 7.09 - 7.11, (2H, t, J_{HH} = 6.4 Hz, H_b), 7.00 - 7.08 (m, 12H, H_g and H_h), 6.93 (t, 2H, J_{HH} =7.6 Hz, H_c), 6.90 (d, 2H, J_{HH} = 8.8 Hz, H_d), 6.31 (s, 2H, H_k), 5.84 (s, 4H, H_i), 1.82 (s, 12H, H_j). ¹³C NMR (150 MHz, C₆D₆, 298K): δ 162.5, 151.20, 146.26, 142.97, 136.83, 131.11, 130.94, 129.21, 129.14, 128.98, 128.19, 127.92, 126.96, 126.75, 126.44, 126.20, 125.55, 121.99, 95.52. 20.37.

Figure 7. Assignment of ¹H NMR signals for 5 (see previous paragraph for details).

Cr[OO]Ph(N₂CPh₂)₂ (6). A (5 mL) THF solution of $Cr_2([OO]^{Ph})_2$ (0.030 g, 0.023 mmol) was reacted with diphenyldiazomethane (0.018 g, 0.092 mmol) for 4 h. The light green color of the complex changed immediately to purple. The solution was stirred for 6 h at RT. The solvent was removed under vacuum and the residue was recrystallized from ether-THF mixture at -35 °C. Brown color crystals were isolated in 52% yield (0.025 g, 0.024 mmol). Calcd for $Cr_0H_{52}Cr_1N_4O_2\times C_4H_8O\times 0.5C_6H_{12}$: C, 80.60, H, 5.80. Found C, 79.52, H, 5.57.

6,6,12,12-tetraphenyl-6,12-dihydroindeno[1,2-b]fluorene (7). 1. Reaction of Cr₂([OO]^{Ph})₂ with

(NO)(BF₄): A solution of (NO)(BF₄) (0.010 g, 0.093 mmol) in THF (5 mL) was added to a THF solution (5 mL) of $Cr_2([OO]^{Ph})_2$ (0.030 g, 0.023 mmol). The green color solution became cloudy and turned yellow over the course of 6 h. The solvent was removed under vacuum and the residue recrystallized with ether-THF mixture. Colorless crystals were obtained in 92% yield (0.023 g, 0.040 mmol). 2. Reaction of $H_2[OO]^{Ph}$ with (NO)(BF₄): A solution of (NO)(BF₄) (0.012 g, 0.1 mmol) in THF (5 mL) was added to a THF solution (5 mL) of $H_2[OO]^{Ph}$ (0.030 g, 0.051 mmol). The colorless solution turned light brown over a period of 6 h. The solvent was removed under vacuum and the residue recrystallized in CH_2Cl_2 . Colorless crystals of 7 were obtained in 77% yield (0.021 g, 0.039 mmol). 1H NMR (600 MHz, CD_2Cl_2 , 298 K): δ 7.81 (s, 2H, He), 7.71 (d, J_{HH} = 7.6 Hz, 2H, H_a), 7.38 (d, 2H, J_{HH} = 7.6, H_d), 7.32 (t, 2H, J_{HH} = 7.6 Hz, H_b), 7.26 (m, 22H, H_c, H_f, H_g, H_h). Related compound (lacking the phenyl substituents) and its NMR characterization were previously reported [50]. ^{13}C NMR (125 MHz, CD_2Cl_2 , 298K): δ 151.48, 151.12, 145.92, 140.21, 139.93, 128.27, 128.13, 127.58, 127.48, 126.69, 126.07, 120.16, 117.81, 65.24. HRMS (m/z): Calcd, $[C_{44}H_{30}]^+$ 558.2347, found 558.2333.

341

Figure 6. Assignment of ¹H NMR signals for 7 (see previous paragraph for details).

342343

344

345

346

347

348

349

350

351

352

353

354

355

356

357

358

359

360

361

362

363

364

365

366

367

368

369

General Procedure for Catalytic Studies. C_6D_6 solution containing 20 equivalents of an organoazide, 24 equivalents of an isocyanide and 2 equivalents of 1,3,5-trimethoxybenzene (internal standard) was mixed with 2.5 mol% catalyst in C_6D_6 . The reaction was heated at 60 °C for 24 h. The products were identified and the yields were calculated using 1H NMR spectroscopy.

3.3. X-ray Crystallographic Details

Structures of complexes 1, 2, 3, and 6, and 6,6,12,12-tetraphenyl-6,12-dihydroindeno-[1,2-b]fluorene (7) were confirmed by X-ray structure determination; data collection and refinement details are given in Table 1. The crystals were mounted on a Bruker APEXII/Kappa three circle goniometer platform diffractometer equipped with an APEX-2 detector. The structures of 1, 3, 6, and 7 were collected using MoK α (λ = 0.71073 Å) at Wayne State University. The structure of 2 was collected using CuKα radiation (1.54178 Å) in the Center for Crystallographic Research in the Department of Chemistry, Michigan State University. The data were processed and refined using the APEX2 software. Structures were solved by direct methods in SHELXS and refined by standard difference Fourier techniques in the SHELXTL program suite (6.10 v., Sheldrick G. M., and Siemens Industrial Automation, 2000). Hydrogen atoms were placed in calculated positions using the standard riding model and refined isotropically; all other atoms were refined anisotropically. The structure of 6 contained half a molecule of cyclohexane and a molecule of THF in the asymmetric unit. The structure of 7 co-crystallized with CH₂Cl₂ which was fully refined. The structure of 3 contained multiple severely disordered THF solvent molecules in the asymmetric unit, leading to the overall poor quality of the diffraction data. We had only limited success in modelling the disorder in THF solvent, thus, SQUEEZE program was applied to remove the disordered solvent. One of the para-tolyl groups in the structure of 3 was found to be disordered; the disorder was successfully modeled by finding two alternative conformations. The structure of 1 was also of relatively poor quality, due to the very small size of the crystals. Despite data collection at 60 s per frame, little diffraction was observed beyond ~1 Å. The structure of 1 contained several toluene molecules per asymmetric unit, one of which was found to be disordered over two conformations. The structure of 2 contained significant amount of highly disordered THF solvent, which was removed using SQUEEZE.

374

375

376

377

378

379

380

381

382

383

384

385

386

387

388

389

390

391

392

393

394

395

396

397

398

399

400

Table 1. X-ray crystallographic details for complexes **1-3**, **6**, and compound **7**.

Complex	1	2	3	6	7
formula	C52H46CrO4×2.5C7H8	2C88H64Cr2O4	C58H46CrN2O2	C ₇₀ H ₅₂ CrN ₄ O ₂ ×0.5C ₆ H ₁₂ ×C ₄ H ₈ O	C22H15×CH2Cl2
fw, g/mol	1020.25	2578.80	854.97	1147.34	364.27
crystal system	Triclinic	Triclinic	Monoclinic	Triclinic	Triclinic
space group	P-1	P-1	P21/c	P-1	P-1
a (Å)	9.946(11)	13.9851(4)	17.38(15)	10.1831(6)	8.7464(5)
b (Å)	14.298(16))	19.4602(6)	13.03(11)	13.0107(7)	8.7610(5)
c (Å)	19.19(2)	30.4287(10)	28.58(19)	23.0961(13)	12.4072(7)
α (deg)	83.38(3)	81.683(2)	90.00	100.964(3)	76.995(2)
β (deg)	82.55(2)	77.609(2)	127.4(4)	101.580(3)	78.928(2)
γ (deg)	82.44(2)	74.125(2)	90.00	99.999(3)	70.505(2)
$V(\mathring{\mathrm{A}}^3)$	2668(5)	7747.2(4)	5142(71)	2870.7(3)	866.13(9)
Z	2	4	4	2	2
d_{calcd} , g/cm^3	1.270	1.1055	1.104	1.327	1.397
μ , mm $^{ ext{-}1}$	0.266	2.673	0.263	0.257	0.377
T(K)	100(2)	172.99	100(2)	100(2)	100(2)
2θ , deg	49.00	128.14	47.44	52.96	55.02
R_{1^a} [(I>2 σ)]	0.0981	0.0827	0.0727	0.0730	0.0388
$wR_{2^b}[(I>2\sigma)]$	0.2070	0.1875	0.1512	0.1710	0.0803
GOF ^c (F ²)	0.973	0.7573	0.881	1.037	1.041

 $^{a}R_{1} = \sum ||F_{0} - F_{c}||/\sum |F_{0}|$. $^{b}wR_{2} = (\sum (w(F_{0}^{2} - F_{c}^{2})^{2})/\sum (w(F_{0}^{2})^{2}))^{1/2}$. $^{c}GOF = (\sum w(F_{0}^{2} - F_{c}^{2})^{2}/(n-p))^{1/2}$ where n is the number of data and p is the number of parameters refined.

3.4. Computational Details

DFT calculations were performed using Gaussian 09 [52]. All calculations were performed at the BP86-D3/def2-SVP level of theory [53–57], employing density fitting, ultrafine grids [58], and Becke-Johnson damping for the dispersion corrections. Optimized structures were confirmed to be minima by ensuring all harmonic frequencies were real. All wavefunctions were verified to be stable. Orbital analyses were performed in GaussView 6.0.16 [59], and Mayer bond orders were calculated using Multiwfn 3.5 [60].

4. Conclusions

We have demonstrated that chelating bis(alkoxide) ligand [OO]^{Ph}, featuring terphenyl spacer between the alkoxide donors, forms mononuclear (Cr[OO]Ph(THF)2) or dinuclear (Cr2[OO]Ph2) Cr(II) complexes, depending on the crystallization conditions. These results suggest that [OO]Ph exhibits larger steric profile compared with two monodentate alkoxides [OC+Bu2Ph], which formed Cr₂(OC^tBu₂Ph)₄ dimer invariably. Reactions with organoazides form diamagnetic Cr(VI) bis(imido) complexes, or paramagnetic Cr(IV) mono(imido) complexes. The outcome of the reaction depends on the sterics of organoazide: while mesityl azide formed Cr(IV) mono(imido), and 3,5-dimethylphenyl/4-methylphenyl azides formed Cr(VI) bis(imido) complexes. With diphenyldiazomethane, chromium bis(diphenylmethylenehydrazido) product forms. Treatment of the Cr(II) precursor with isocyanide likely forms a Cr(II) isocyanide adduct, whereas no reaction is observed with CO. Isoelectronic nitrosonium abstracts hydroxyl to induce cyclization producing 6,6,12,12-tetraphenyl-6,12-dihydroindeno[1,2-b]fluorene. Catalytic studies combining mixtures of isocyanides with organozides enable carbodiimide formation only for bulkier (mono- or di-orthosubstituted) aryl azides. This finding is consistent with our previous report, that demonstrated that the C-N bond formation in carbodiimide is preceded by isocyanide coordination to the metal and thus occurs at Cr(IV) mono(imido) intermediate only. Our future studies will focus on the development of new chelating bis(alkoxide) ligands which could enable catalytic reactivity for wider range of substrates.

- 401 **Supplementary Materials:** The following are available online at www.mdpi.com/xxx/s1: NMR, MS, UV-vis and
- 402 IR spectra, cif files, and computational details. Cif files of the structures of 1-3, 6, and 7 were deposited at CCDC
- 403 under the following numbers: 1970958-1970562.
- 404 Author Contributions: Conceptualization: SSK, RLL, SG; methodology: SSK, RJS, RLL, SG; writing—original
- draft preparation, SSK, RLL, SG; writing—review and editing, SSK, RLL; supervision: RLL, SG; funding
- 406 acquisition: RLL, SG, RJS.
- 407 Funding: This research was funded by National Science Foundation, Division of Chemistry, grant number CHE
- 408 1855681.
- 409 **Acknowledgments:** Compounds characterization was carried out at Lumigen Instrument Center, Wayne State
- 410 University. The CCD based x-ray diffractometer at Michigan State University were upgraded and/or replaced
- 411 by departmental funds. We thank Amanda Grass and Duleeka Sudheer for technical assistance.
- 412 **Conflicts of Interest:** The authors declare no conflict of interest.

413 References

- 414 1. Jenkins, D.M. Atom-Economical C2 + N1 Aziridination: Progress towards Catalytic Intermolecular Reactions Using Alkenes and Aryl Azides. *Synlett* **2012**, 23, 1267–1270.
- Driver, T.G. Recent Advances in Transition Metal-Catalyzed N-Atom Transfer Reactions of Azides. *Org. Biomol. Chem.* 2010, *8*, 3831–3846.
- 3. Shin, K.; Kim, H.; Chang, S. Transition-Metal-Catalyzed C-N Bond Forming Reactions Using Organic Azides as the Nitrogen Source: A Journey for the Mild and Versatile C-H Amination. *Acc. Chem. Res.* **2015**, 48, 1040–1052.
- 421 4. Wang, P.; Deng, L. Recent Advances in Iron-Catalyzed C-H Bond Amination via Iron Imido Intermediate. *Chin. J. Chem.* **2018**, *36*, 1222–1240.
- Lu, H.; Zhang, X.P. Catalytic C–H functionalization by metalloporphyrins: Recent developments and future directions. *Chem. Soc. Rev.* **2011**, *40*, 1899–1909.
- 425 6. Uchida, T.; Katsuki, T. Asymmetric Nitrene Transfer Reactions: Sulfimidation, Aziridination and C–H Amination Using Azide Compounds as Nitrene Precursors. *Chem. Rec.* **2014**, *14*, 117–129.
- 427 7. Kuijpers, P.F.; van der Vlugt, J.I.; Schneider, S.; de Bruin, B. Nitrene Radical Intermediates in Catalytic Synthesis. *Chem. Eur. J.* **2017**, *23*, 13819–13829.
- 429 8. Baek, Y.; Hennessy, E.T.; Betley, T.A. Direct Manipulation of Metal Imido Geometry: Key Principles to Enhance C–H Amination Efficacy. *J. Am. Chem. Soc.* **2019**, *141*, 16944–16953.
- 431 9. Wilding, M.J.T.; Iovan, D.A.; Betley, T.A. J. Am. Chem. Soc. 2017, 139, 12043–12049.
- 432 10. Cheng, J.; Liu, J.; Leng, X.; Lohmiller, T.; Schnegg, A.; Bill, E.; Ye, S.; Deng, L. A Two-Coordinate Iron(II)
 433 Imido Complex with NHC Ligation: Synthesis, Characterization, and Its Diversified Reactivity of Nitrene
 434 Transfer and C–H Bond Activation. *Inorg. Chem.* **2019**, *58*, 7634-7644.
- 435 11. Du, J.; Wang, L.; Xie, M.; Deng, L. A Two-Coordinate Cobalt(II) Imido Complex with NHC Ligation: Synthesis, Structure, and Reactivity. *Angew. Chem. Int. Ed.*, **2015**, 54, 12640–12644.
- 437 12. Cowley, R.E.; Golder, M.R.; Eckert, N.A.; Al-Afyouni, M.H.; Holland, P.L. Mechanism of Catalytic Nitrene 438 Transfer using Iron(I)-Isocyanide Complexes. *Organometallics* **2013**, 32, 5289–5298.
- 439 13. Bagh, B.; Broere, D.L.J.; Sinha, V.; Kuijpers, P.F.; van Leest, N.P.; de Bruin, B.; Demeshko, S.; Siegler, M.A.; van der Vlugt, J.I. Catalytic Synthesis of N-Heterocycles via Direct C(sp3)–H Amination Using an Air-Stable Iron(III) Species with a Redox-Active Ligand, J. Am. Chem. Soc. **2017**, *139*, 5117-5124.
- 442 14. Vreeken, V.; Baij, L.; de Bruin, B.; Siegler, M.A.; van der Vlugt, J.I. N-Atom transfer via thermal or photolytic activation of a Co-azido complex with a PNP pincer ligand. *Dalton Trans.* **2017**, *46*, 7145–7149.
- Hakey, B.M.; Darmon, J.M.; Akhmedov, N.G.; Petersen, J.L.; Milsmann, C. Reactivity of Pyridine Dipyrrolide Iron(II) Complexes with Organic Azides: C–H Amination and Iron Tetrazene Formation. *Inorg. Chem.* 2019, *58*, 11028–11042.
- 447 16. Goswami, M.; de Bruin, B. Porphyrin Co(III)-Nitrene Radical Mediated Pathway for Synthesis of o-Aminoazobenzenes. *Molecules* **2018**, *23*, 1052. (https://doi.org/10.3390/molecules23051052).
- 449 Mankad, N.P.; Müller, P.; Peters, J.C. Catalytic N-N Coupling of Aryl Azides To Yield Azoarenes via 450 Trigonal Bipyramid Iron-Nitrene Intermediates. *J. Am. Chem. Soc.* **2010**, *132*, 4083–4085.

- 451 18. Lang, K.; Torker, S.; Wojtas, L.; Zhang, X.P. Asymmetric Induction and Enantiodivergence in Catalytic Radical C–H Amination via Enantiodifferentiative H-Atom Abstraction and Stereoretentive Radical Substitution. *J. Am. Chem. Soc.* **2019**, *141*, 12388–12396.
- 454 19. Jacobs, B.P.; Wolczanski, P.T.; Jiang, Q.; Cundari, T.R.; MacMillan, S.N. Rare Examples of Fe(IV) Alkyl-Imide Migratory Insertions: Impact of Fe-C Covalency in (Me₂IPr)Fe(=NAd)R₂ (R = neoPe, 1-nor). *J. Am. Chem. Soc.* **2017**, 139, 12145–12148.
- 457 20. Powers, I.G.; Andjaba, J.M.; Luo, X.; Mei, J.; Uyeda, C. Catalytic Azoarene Synthesis from Aryl Azides Enabled by a Dinuclear Ni Complex. *J. Am. Chem. Soc.* **2018**, *140*, 4110-4118.
- 459 21. Spasyuk, D.M.; Carpenter, S.H.; Kefalidis, C.E.; Piers, W.E.; Neidig, M.L.; Maron, L. Facile Hydrogen 460 Atom Transfer to Iron(III) Imido Radical Complexes Supported by a Dianionic Pentadentate Ligand. 461 *Chem. Sci.* **2016**, *7*, 5939–5944.
- 462 22. Nugent, W.A.; Mayer, J.M. Metal-Ligand Multiple Bonds: The Chemistry of Transition Metal Complexes Containing Oxo, Nitrido, Imido, Alkylidene, or Alkylidyne Ligands. 1st Edition, Wiley-Interscience, 1988.`.
- 464 23. Danopoulos, A.A.; Hussain-Bates, B.; Hursthouse, M.B.; Leung, W.H.; Wilkinson, G.; t-Butylimido complexes of chromium(V). X-Ray Crystal Structure of t-Butylimidotrichlorobis(ethyldiphenylphosphine)chromium(V). J. Chem. Soc., Chem. Commun. 1990, 23, 1678–1679.
- 468 24. Danopoulos, A.A.; Hankin, D.M.; Wilkinson, G.; Cafferkey, S.M.; Sweet, T.K.N.; Hursthouse, M.B.; 469 Amido, Imido and Carbene Complexes of Chromium. *Polyhedron* 1997, 16, 3879–3892.
- 470 25. Edwards, N.Y.; Eikey, R.A.; Loring, M.I.; Abu-Omar, M.M.; High-Valent Imido Complexes of Manganese and Chromium Corroles. *Inorg. Chem.* **2005**, *44*, 3700-3708.
- 472 26. Wu, P.; Yap, G.P.A.; Theopold, K.H. Structure and Reactivity of Chromium(VI) Alkylidenes. *J. Am. Chem.* 473 Soc. **2018**, 140, 7088-7091.
- 474 27. Leung, W.-H. Synthesis and Reactivity of Organoimido Complexes of Chromium, *Eur. J. Inorg. Chem.* **2003**, 583-593.
- 476 28. Beaumier, E.P.; Billow, B.S.; Singh, A.K.; Biros, S.M.; Odom, A.L. A complex with nitrogen single, double, and triple bonds to the same chromium atom: Synthesis, structure, and reactivity, *Chem. Sci.* **2016**, 7, 2532–2539.
- 479 29. Keller, C.L.; Kern, J.L.; Terry, B.D.; Roy, S.; Jenkins, D.M., Catalytic aziridination with alcoholic substrates via a chromium tetracarbene catalyst. *Chem. Commun.* **2018**, *54*, 1429–1432.
- 481 30. Elpitiya, G.R.; Malbrecht, B.J.; Jenkins, D.M., A Chromium(II) Tetracarbene Complex Allows Unprecedented Oxidative Group Transfer. *Inorg. Chem.* **2017**, *56*, 14101–14110.
- 483 31. Yousif, M.; Tjapkes, D.J.; Lord, R.L.; Groysman, S. Catalytic Formation of Asymmetric Carbodiimides at Mononuclear Chromium (II/IV) Bis(alkoxide) Complexes. *Organometallics* **2015**, *34*, 5119–5128.
- 485 32. Heins, S.P.; Morris, W.D.; Wolczanski, P.T.; Lobkovsky, E.B.; Cundari, T.R. Nitrene Insertion into C-C and C-H Bonds of Diamide Diimine Ligands Ligated to Chromium and Iron. *Angew. Chem. Int. Ed.* **2015**, *54*, 14407–14411.
- 488 33. Bellow, J.A.; Yousif, M.; Groysman, S. Discrete Complexes of 3d Metals with Monodentate Bulky Alkoxide Ligands and Their Reactivity in Bond Activation and Bond Formation Reactions. *Comments Inorg. Chem.* 490 2015, 36, 92–122.
- 491 34. Grass, A.; Wannipurage, D.; Lord, R.L.; Groysman, S. Group-transfer chemistry at transition metal centers in bulky alkoxide ligand environments. *Coord. Chem. Rev.* **2019**, *400*, 1–16.
- 493 35. Kurup, S.S.; Wannipurage, D.; Lord, R.L.; Groysman, S. An iron complex with a new chelating bis(alkoxide) ligand leads to an active nitrene dimerization catalyst for a variety of para- and meta-substituted azide precursors. *Chem. Commun.* **2019**, *55*, 10780–10783.
- 496 36. Yousif, M.; Wannipurage, D.; Huizenga, C.D.; Washnock-Schmid, E.; Peraino, N.J.; Ozarowski, A.; Stoian, S.A.; Lord, R.L.; Groysman, S. Catalytic Nitrene Homocoupling by an Iron(II) Bis(alkoxide) Complex: Bulking Up the Alkoxide Enables a Wider Range of Substrates and Provides Insight into the Reaction Mechanism. *Inorg. Chem.* 2018, 57, 9425–9438.
- 500 37. Bellow, J.A.; Yousif, M.; Cabelof, A.C.; Lord, R.L.; Groysman, S. Reactivity Modes of an Iron Bis(alkoxide) 501 Complex with Aryl Azides: Catalytic Nitrene Coupling vs Formation of Iron(III) Imido Dimers. 502 Organometallics **2015**, *34*, 2917–2923.

- 503 38. Yousif, M.; Cabelof, A.C.; Martin, P.D.; Lord, R.L.; Groysman, S. Synthesis of a Mononuclear, Non-Square-Planar Chromium(II) Bis(alkoxide) Complex and its Reactivity Toward Organic Carbonyls and CO₂. Dalton Trans. **2016**, 45, 9794–9804.
- 506 39. Murray, B.D.; Hope, H.; Power, P.P. An Unusual C-C Bond Cleavage in a Bulky Metal Alkoxide: Syntheses and X-ray Crystal Structures of Three-Coordinate Mn(II) and Cr(II) Complexes Containing the Di-tert-butylmethoxide Ligand. *J. Am. Chem. Soc.* 1985, 107, 169–173.
- 509 40. Sydora, O.L.; Kuiper, D.S.; Wolczanski, P.T.; Lobkovsky, E.B.; Dinescu, A.; Cundari, T.R. The Butterfly Dimer [(tBu3SiO)Cr]2(μ -OSitBu3)2 and Its Oxidative Cleavage to (tBu3SiO)2Cr(N-NCPh2)2 and (tBu3SiO)2CrN(2,6-Ph2-C6H3). *Inorg. Chem.* 2006, 45, 2008–2021.
- 512 41. Ohki, Y.; Takikawa, Y.; Hatanaka, T.; Tatsumi, K. Reductive N–N Bond Cleavage of Diphenylhydrazine and Azobenzene Induced by Coordinatively Unsaturated Cp*Fe{N(SiMe3)2}. *Organometallics* **2006**, 25, 3111–3113.
- 515 42. Bellows, S.M.; Arnet, N.A.; Gurubasavaraj, P.M.; Brennessel, W.W.; Bill, E.; Cundari, T.R.; Holland, P.L. The Mechanism of N-N Double Bond Cleavage by an Iron(II)-Hydride Complex. *J. Am. Chem Soc.* **2016**, 138, 12112–12123.
- 518 43. Davis-Gilbert, Z.W.; Wen, X.; Goodpaster, J.D.; Tonks, I.A. Mechanism of Ti-Catalyzed Oxidative Nitrene 519 Transfer in [2 + 2 + 1] Pyrrole Synthesis from Alkynes and Azobenzene. J Am Chem Soc. **2018**, *140*, 7267– 520 7281.
- 521 44. Kawakita, K.; Beaumier, E.P.; Kakiuchi, Y.; Tsurugi, H.; Tonks, I.A.; Mashima, K. 522 Bis(imido)vanadium(V)-Catalyzed [2+2+1] Coupling of Alkynes and Azobenzenes Giving Multisubstituted Pyrroles. J. Am. Chem. Soc. 2019, 141, 4194–4198.
- 524 45. Copéret, C.; Comas-Vives, A.; Conley, M.P.; Estes, D.P.; Fedorov, A.; Mougel, V.; Nagae, H.; Núñez-Zarur, 525 F.; P. A. Zhizhko. Surface Organometallic and Coordination Chemistry toward Single-Site Heterogeneous 526 Catalysts: Strategies, Methods, Structures, and Activities. *Chem. Rev.* 2016, 116, 323–421.
- 527 46. Wu, P.; Yap, G.P.A.; Theopold, K.H. Synthesis, Characterization, and Reactivity of Chromium(VI) 528 Alkylidenes, *Organometallics* **2019**, *38*, 4593–4600.
- 529 47. Grass, A.; Dewey. N. S.; Lord, R.L.; Groysman, S. Ketenimine Formation Catalyzed by a High Valent Cobalt Carbene in Bulky Alkoxide Ligand Environment, *Organometallics* **2019**, *38*, 962–972.
- 531 48. Grass, A.; Stoian, S.A.; Lord, R.L.; Groysman, S. Transition metal-mediated reductive coupling of diazoesters, *Chem. Commun.* **2019**, *55*, 8458–8461.
- 533 49. Hempe, M.; Reggelin, M. Molecular Packing and Morphological Stability of Dihydro-indeno[1,2-b]fluorenes in the Context of Their substitution Pattern, RSC Adv. 2017, 7, 47183–47189.
- 536 50. Poriel, C.; Liang, J.-J.; Rault-Berthelot, J.; Barrière, F.; Cocherel, N.; Slawin, A.M.Z.; Horhant, D.; Virboul, M.; Alcaraz, G.; Audebrand, N.; et al. Dispirofluorene–Indenofluorene Derivatives as New Building Blocks for Blue Organic Electroluminescent Devices and Electroactive Polymers. *Chem. Eur. J.* 2007, 13, 10055–10069.
- 540 51. Bradley, D.C.; Hursthouse, M.B.; Newing, C.W.; Welch, A. Square planar and tetrahedral chromium(II) complexes; crystal structure determinations. *J. Chem. Soc., Chem. Commun.* **1972**, 567–568.
- 542 52. Frisch, M.J.; Trucks, G.W.; Schlegel, H.B.; Scuseria, G.E.; et al. Gaussian 09W, revision D.01; Gaussian, Inc.: Wallingford, CT, USA, 2009.
- 544 53. Becke, A.D. Density-functional exchange-energy approximation with correct asymptotic behavior. *Phys.* 545 *Rev. A.* **1988**, *38*, 3098–3100.
- 546 54. Perdew, J.P. Density-functional approximation for the correlation energy of the inhomogeneous electron gas. *Phys. Rev. B.* **1986**, 33, 8822–8824.
- 548 55. Grimme, S.; Antony, J.; Ehrlich, S.; Krieg, H. A consistent and accurate ab initio parameterization of density functional dispersion correction (DFT-D) for the 94 elements H–Pu. *J. Chem. Phys.* **2010**, *132*, 154104.
- 551 56. Grimme, S.; Ehrlich, S.; Goerigk, L. Effect of the damping function in dispersion corrected density functional theory. *J. Comput. Chem.* **2011**, 32, 1456–1465.
- 553 57. Weigend, F.; Ahlrichs, R. Balanced basis sets of split valence, triple zeta valence, and quadruple zeta valence quality for H to Rn: Design and assessment of accuracy. *Phys. Chem. Chem. Phys.* **2005**, *7*, 3297–3305.

- 556 58. Bootsma, A.N.; Wheeler, S. Popular Integration Grids Can Result in Large Errors in DFT-Computed Free Energies. *ChemRxiv* **2019**, *Preprint*, https://doi.org/10.26434/chemrxiv.8864204.v5.
- 558 59. GaussView Version 6, Dennington, R.; Keith, T.A.; Millam, J.M. Semichem Inc., Shawnee Mission, KS, 2016.
- 560 60. Lu, T.; Chen, F. Multiwfn: A multifunctional wavefunction analyzer. *J. Comput. Chem.* **2012**, *33*, 580–592.



© 2020 by the authors. Submitted for possible open access publication under the terms and conditions of the Creative Commons Attribution (CC BY) license (http://creativecommons.org/licenses/by/4.0/).